Current Eye Research

ISSN: (Print) (Online) Journal homepage: https://www.tandfonline.com/loi/icey20

# Research on Assistant Diagnosis of Fundus Optic Neuropathy Based on Deep Learning

Chengjin Wang, Yuwei Zhang, Shuai Xu, Yuyan Liu, Lindan Xie, Changlong Wu, Qianhui Yang, Yanhua Chu & Qing Ye

**To cite this article:** Chengjin Wang, Yuwei Zhang, Shuai Xu, Yuyan Liu, Lindan Xie, Changlong Wu, Qianhui Yang, Yanhua Chu & Qing Ye (2022): Research on Assistant Diagnosis of Fundus Optic Neuropathy Based on Deep Learning, Current Eye Research, DOI: 10.1080/02713683.2022.2138917

**To link to this article:** https://doi.org/10.1080/02713683.2022.2138917

Published online: 27 Oct 2022.

CURRENT EYE RESEARCH
https://doi.org/10.1080/02713683.2022.2138917



# Research on Assistant Diagnosis of Fundus Optic Neuropathy Based on Deep Learning

Chengjin Wang[a*], Yuwei Zhang[a*], Shuai Xu[a], Yuyan Liu[b], Lindan Xie[b], Changlong Wu[c], Qianhui Yang[d], Yanhua Chu[b], and Qing Ye[a,e]

[a]Key Laboratory of Weak-Light Nonlinear Photonics, School of Physics and TEDA Applied Physics, Ministry of Education, Nankai University, Tianjin, China; [b]Tianjin Key Lab of Ophthalmology and Visual Science, Tianjin Eye Hospital and Eye Institute, Nankai University Affiliated Eye Hospital, Clinical College of Ophthalmology Tianjin Medical University, Tianjin, China; [c]Ophthalmology, Jinan Second People's Hospital, Jinan City, Shandong Province, China; [d]Tianjin Key Laboratory of Retinal Functions and Diseases, Tianjin Branch of National Clinical Research Center for Ocular Disease, Eye Institute and School of Optometry, Tianjin Medical University Eye Hospital, Tianjin, China; [e]Nankai University Eye Institute, Nankai University Afflicted Eye Hospital, Nankai University, Tianjin, China

**ABSTRACT**

**Purpose:** The purpose of this study was to use the neural network to distinguish optic edema (ODE), and optic atrophy from normal fundus images and try to use visualization to explain the artificial intelligence methods.

**Methods:** Three hundred and sixty-seven images of ODE, 206 images of optic atrophy, and 231 images of normal fundus were used, which were provided by two hospitals. A set of image preprocessing and data enhancement methods were created and a variety of different neural network models, such as VGG16, VGG19, Inception V3, and 50-layer Deep Residual Learning (ResNet50) were used. The accuracy, recall, F1-score, and ROC curve under different networks were analyzed to evaluate the performance of models. Besides, CAM (class activation mapping) was utilized to find the focus of neural network and visualization of neural network with feature fusion.

**Results:** Our image preprocessing and data enhancement method significantly improved the accuracy of model performance by about 10%. Among the networks, VGG16 had the best effect, as the accuracy of ODE, optic atrophy and normal fundus were 98, 90, and 95%, respectively. The macro-average and micro-average of VGG16 both reached 0.98. From CAM we can clearly find out that the focus area of the network is near the optic cup. From feature fusion images, we can find out the difference between the three types fundus images.

**Conclusion:** Through image preprocessing, data enhancement, and neural network training, we applied artificial intelligence to identify ophthalmic diseases, acquired the focus area through CAM, and identified the difference between the three ophthalmic diseases through neural network middle layers visualization. With the help of assistant diagnosis, ophthalmologists can evaluate cases more precisely and more clearly.

**ARTICLE HISTORY**
Received 19 August 2022
Accepted 18 October 2022

**KEYWORDS**
Deep learning; convolutional neural network; visualization; CAM; funds photos

## Introduction

Roughly, the optic nerve can be divided into four parts: the intraocular segment, the intraorbital segment, the canalicular segment, and the intracranial segment. As the anterior surface of the intraocular segment, that is the optic nerve head (ONH), is the only part that can be clinically visible through direct or indirect ophthalmoscopy, it is essential for ophthalmologists to screen and assess the appearance of ONH.[1–4]

Many conditions would cause abnormalities of the ONH. The common manifestations include papilledema, optic disk edema (ODE), optic atrophy, and congenital abnormalities of ONH. Among them, congenital anomalies of the optic nerve are relatively stable, while ODE and optic atrophy might be occult at onset, progressive aggravation, and even related to a variety of vision-threatening or life-threatening disorders. It is of great clinical significance for the early detection and diagnosis of these signs while those devastating diseases are highly suspicious. At present, there are few neuro-ophthalmological specialists, especially in grass-roots hospitals. Therefore, the development and application of optic nerve disease recognition software based on fundus photography results have important clinical significance and broad application prospects.

The automatic detection method for fundus diseases consists of two parts, image treatment, and classifier. Generally, fundus images need to be resized and denoized to highlight the key parts, and image features need to be extracted. Then classifiers can divide images into different categories.

CONTACT Yanhua Chu chuchutj@126.com Tianjin Key Lab of Ophthalmology and Visual Science, Tianjin Eye Hospital and Eye Institute, Nankai University Affiliated Eye Hospital, Clinical College of Ophthalmology Tianjin Medical University, Tianjin, China; Qing Ye yeqing@nankai.edu.cn Key Laboratory of Weak-Light Nonlinear Photonics, School of Physics and TEDA Applied Physics, Ministry of Education, Nankai University, Tianjin, China
*These authors have contributed equally to this work.

In 2016, Gulshan proposed to use the artificial intelligence (AI) system of deep learning (DL) to recognize fundus images to diabetic retinopathy (DR). Studies have proven that the DL algorithm has high sensitivity and specificity for detecting DR, but the feasibility and accuracy of the algorithm in the real clinical environment need to be further studied.[5] In 2017, Gargeya used a convolution neural network to train 75,137 public fundus images of diabetes patients, achieved 0.97 AUC, and can independently identify and judge cases that should be referred to ophthalmologists for evaluation and treatment.[6] In 2019, Wang created a deep learning system that can distinguish more than 30 types of fundus states.[7] Lakshmana[8] and Sarmad[9] used different methods to process image to make blood vessels segmented, which extracted important features. Lakshmana[8] and Venkatesan[10] both extracted textural gray-level features and used them as input to the classifier and each accuracy of traditional methods is more than 90%. Compared with traditional algorithms, convolution neural network classifies the input image through convolution, pool, and full connection layers, which greatly reduces the workload of extracting image features.[11–13] While every step of traditional methods is purposeful and interpretable, besides it is easy to visualize its processing.

Although the neural network works well, the mechanism and visual exploration of the neural network remains to be found, which means that studies focus on how to use network to distinguish different types of fundus images but lack of interpretation of network. So, we use a neural network to distinguish optic edema (ODE), optic atrophy from normal fundus images to extend its application and combine traditional image algorithms to understand the process of network.

A fully automated neural network algorithm was used for assistant diagnosis of fundus optic neuropathy and the accuracy of final model was high enough to meet the requirements. Especially, the set of images preprocessing and data enhancement we created largely improved the accuracy of networks. Besides, CAM and feature fusion were used to visualize neural networks which allow us to analyze the main focus area of fundus photography and research the intermediate process of neural network. Our assistant diagnosis system achieved the early detection of these optic neuropathies and alleviated the problem of lack of medical resources and provided interpretability for neural networks.

## Methods

### Data preparation

Fundus photos are collected from two hospitals. Tianjin Eye Hospital, Tianjin Key Lab of Ophthalmology and Visual Science, Tianjin Eye Institute, Clinical College of Ophthalmology Tianjin Medical University, Tianjin, China. Jinan Second People's Hospital, Ophthalmology, Jinan City, Shandong Province, China.

A total of 804 images were obtained, including 367 images of ODE, 206 of optic atrophy, and 231 images of the normal optic disk. The images were randomly divided into 644 training sets and 160 test sets. 644 images were used to train the neural network, and 160 images were used to evaluate the final model.

### Patients

Patients with fundus photographs that included the optic disk and definite clinical diagnoses of corresponding optic neuropathy made by expert ophthalmologists according to their medical histories and other diagnostic auxiliary testing were included. To obtain normal fundus photographs, healthy persons and patients without any ocular conditions were also included. Patients with unclear diagnoses or co-existing any other retinopathy and choroidopathy were excluded. The cases who have glaucoma or optic nerve dysplasia corresponding to subjects with damage in the ONH area were excluded.

In this study, the appearances of optic disk were categorized into 3 types: the "normal" appearing optic disk (Figure 1(A)) which was regarded as no abnormalities, both the shape and color, of optic papilla. While ODE (Figure 1(C)) was defined as swelling of the optic papilla regardless of the precise etiologies (intracranial hypertension, inflammatory, ischemic). The "optic atrophy" (Figure 1(B)) was defined as optic disk pale with clinically definite visual dysfunction (impairment of visual acuity, color vision, or present of relative afferent pupillary defect if unilateral).

### Image preprocessing

Due to the different acquisition methods of photos, their brightness and scale storage were not matched, so the images need to be preprocessed to reduce the difference caused by the image format.

For the origin image in Figure 2(A), firstly, the useless black part by automatic clipping was cut out, and only the fundus part was retained as shown in Figure 2(B). Then the image was resized to $512 \times 512$ by biquadratic interpolation to get the clipped photo in Figure 2(C). Although the image was easier to be observed after clipping and zooming, the feature of the fundus photograph was still not obvious. The following methods were adopted to reduce noise and highlight the contrast between blood vessels and other parts. Gaussian filtering was used with the kernel size of 241 and $\sigma$ of 30 to process Figure 2(C) to get Figure 2(D). Because the kernel size and $\sigma$ were too large for the image, important parts were blurred while noise was eliminated. Therefore, they were fused with the following formula:

$$FigE = 4 * FigC - 4 * FigD + 128 \quad (1)$$

By image subtraction, the key vessels were highlighted and the influence of other parts was weakened and the pixel value was shifted upwards, making more pixel values greater than zero. Besides, the pixel value greater than 255 was set to 255, and the pixel value less than 0 was set to zero to limit the range of pixel values. Finally, the obtained image used biquadratic interpolation method again to obtain a 224 $\times$ 224 image (Figure 2(E)). Through image preprocessing,

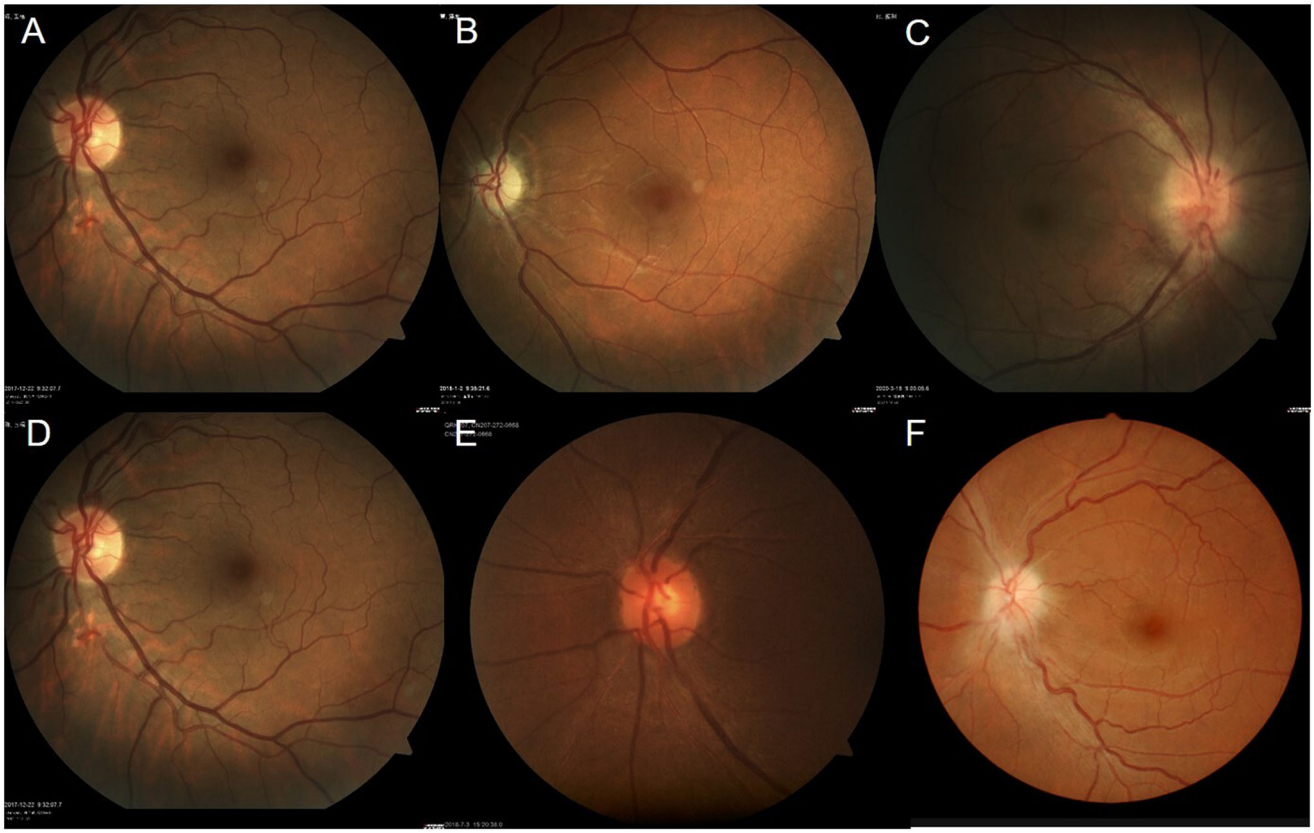


**Figure 1.** Optic disk findings in fundus photography. A, B, and C are three types of images, namely normal optic atrophy and ODE. D, E, and F are three images acquired by the different devices.

the images of different formats were converted into the same format to avoid the impact of different formats.

### Data augmentation

In order to prevent overfitting and limit the number of image samples, the following methods were adopted to enhance the data of the preprocessed image before it is input into the neural network.[14] In this way, in every epoch, the same image would generate a totally new image, but it would still keep the characteristics of the original category, which enables data enhancement.

Our data enhancement method had three aspects, geometric transformation, color transformation and Gaussian noise. The three angles affected an image at the same time, and a new image was finally generated from the set random probability. In terms of geometric transformation, a 50% probability was set to perform horizontal mirror symmetry and vertical mirror symmetry transformation, and a 50% probability was set to crop 0–10% edge row elements or column elements.[15] Besides, a set of affine transformation method included zooming the image to 80–120% of its original size, rotating the image –45° to 45° and shearing the image –25° to 25° randomly. In terms of color transformation, the value of HSV space was changed from 80 to 120% of its original value. In order to improve the robustness of the system, Gaussian noise was added randomly. Through data enhancement, the diversity of image data was increased and overfitting was reduced while retaining the original features.

The flow chart was shown in Figure 2(G). Through image preprocessing of 804 photos, the average and variance of three RGB channels were acquired, which were [0.518, 0.507, 0.502] and [0.219, 0.190, 0.151], respectively. To make the features prominent, after data augmentation, images would subtract the average value and would be divided by the variance, before they were put into the neural network.

### Convolutional neural network

Transfer learning was applied to the neural networks of VGG16, VGG19, Inception V3 and ResNet50, and their full connection layers were modified to satisfy our task.[16] Cross entropy loss was used as the loss function rather than focal loss and Adam as the optimizer.[17,18] Because there was little difference in the number of the three types of fundus images, the advantage of focal loss was hard to be reflected, and the convergence speed of Adam was better than other optimizers. The calculation method of iterating all the parameters through pre-training was adopted. Although it required more computing resources, it could bring better results.

To obtain more appropriate super parameters, different batch sizes and learning rates of different orders of magnitude were used. Finally, the batch size was set to 4, the learning rate was set to 0.0001 and the epoch was set to 100, while the loss function basically converged when epoch was about 50–70. Besides, the Dropout method was used to reduce nodes to prevent from over fitting.

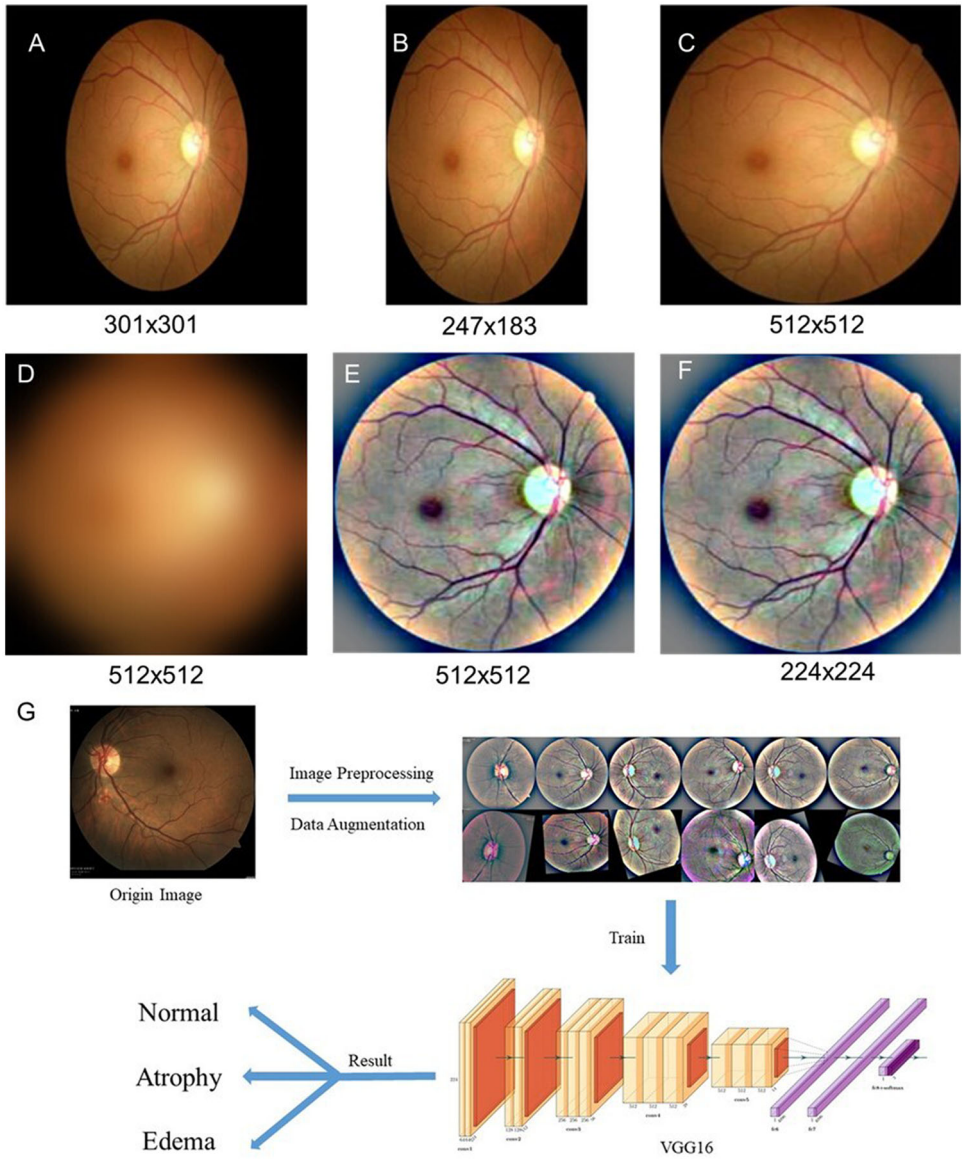


**Figure 2.** Schematic view of image pre-processing process and network training process. A is the original image, B is the image after clipping, C is the image after size change, D is the image after Gaussian blur, E is the image after fusion, and F is the final image after size change, and G is the schematic view of training network. After image preprocessing and data augmentation, images were inputted into networks.

**Table 1.** Evaluation of preprocessing and data enhancement.

| | Without preprocessing | | | Preprocessing | | | Preprocessing and data enhancement | | |
|---|---|---|---|---|---|---|---|---|---|
| Class | Precision | Recall | F1-Score | Precision | Recall | F1-Score | Precision | Recall | F1-Score |
| Normal | 0.88 | 0.71 | 0.79 | 0.90 | 0.95 | 0.92 | 0.95 | 0.96 | 0.95 |
| Atrophy | 0.81 | 0.61 | 0.69 | 0.92 | 0.80 | 0.86 | 0.90 | 0.90 | 0.90 |
| Edema | 0.61 | 0.93 | 0.74 | 0.87 | 0.89 | 0.88 | 0.98 | 0.96 | 0.97 |
| Micro-average | 0.79 | 0.75 | 0.75 | 0.89 | 0.89 | 0.89 | 0.94 | 0.94 | 0.94 |

Through the iterative calculation of convolutional neural network, the accuracy, recall and F1-score of each model were acquired. These indicators were utilized to judge the advantages and disadvantages of neural network structure.

## Results

### *Data augmentation and image preprocessing*

VGG16 was utilized to compare whether to use preprocessing and data enhancement, and the results are shown in Table 1. The effect of the model trained after pretreatment is better than that non pretreatment. The micro-average performance has basically increased by more than 0.1, which is a very significant improvement. The model effect is further improved after data enhancement, which shows that both image preprocessing and data enhancement can significantly improve the model effect.

### *Convolutional neural network*

As shown in Table 2, the accuracy, recall and F1 score of vgg16 were the best under the three categories of edema,

**Table 2.** Evaluation of different neural networks.

| | VGG16 | | | VGG19 | | | ResNet50 | | | Inception V3 | | |
|---|---|---|---|---|---|---|---|---|---|---|---|---|
| Class | Precision | Recall | F1-Score | Precision | Recall | F1-Score | Precision | Recall | F1-Score | Precision | Recall | F1-Score |
| Normal | 0.95 | 0.96 | 0.95 | 0.93 | 0.96 | 0.95 | 0.93 | 0.96 | 0.95 | 0.86 | 0.90 | 0.88 |
| Atrophy | 0.90 | 0.90 | 0.90 | 0.88 | 0.85 | 0.86 | 0.90 | 0.88 | 0.89 | 0.72 | 0.80 | 0.76 |
| Edema | 0.98 | 0.96 | 0.97 | 0.93 | 0.91 | 0.92 | 0.93 | 0.91 | 0.92 | 0.92 | 0.74 | 0.82 |
| Micro-average | 0.94 | 0.94 | 0.94 | 0.92 | 0.92 | 0.92 | 0.92 | 0.93 | 0.92 | 0.84 | 0.83 | 0.83 |

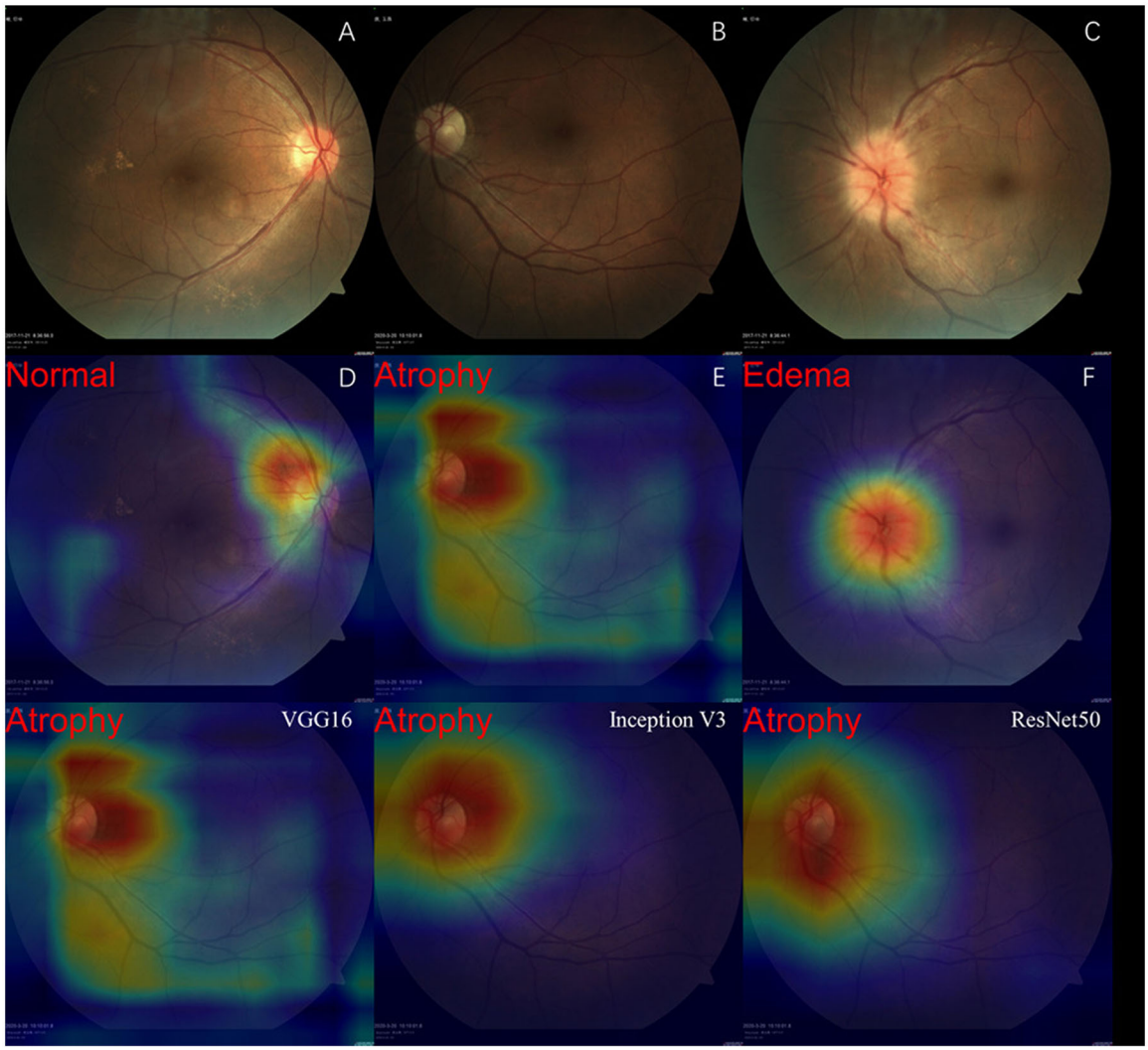


**Figure 3.** Visualization maps generated from neural networks. A, B, and C are the origin images. D, E, and F are CAMs corresponding to the previous line. Images on the third row are CAMs of different neural networks.

normal and atrophy. The network structure of Inception v3 was the most complex one and it had the deepest layers, while its performance was the worst. This showed that for a specific practical problem (fundus photo classification), the more complex the network structure did not mean the better results. Although the standard deviation of ResNet50 was the smallest, its average value was higher than VGG19 but slightly lower than VGG16, besides, each performance of ResNet50 was not higher than VGG16. Therefore, VGG16 was chosen as the best model for fundus optic neuropathy.

The ROC (receiver operating characteristic) curve and confusion matrix of the best model (VGG16) were drawn (as shown in Figure 3). All types of AUC reach more than 0.97, which means the final model is very reliable.

Since the accuracy by using VGG16 model is high enough, we believe that deep learning technology can play an auxiliary role in identifying fundus images and distinguishing ophthalmic diseases.

## Visualization

Although neural networks were used to judge ocular fundus diseases, and the performance is excellent, the explanation

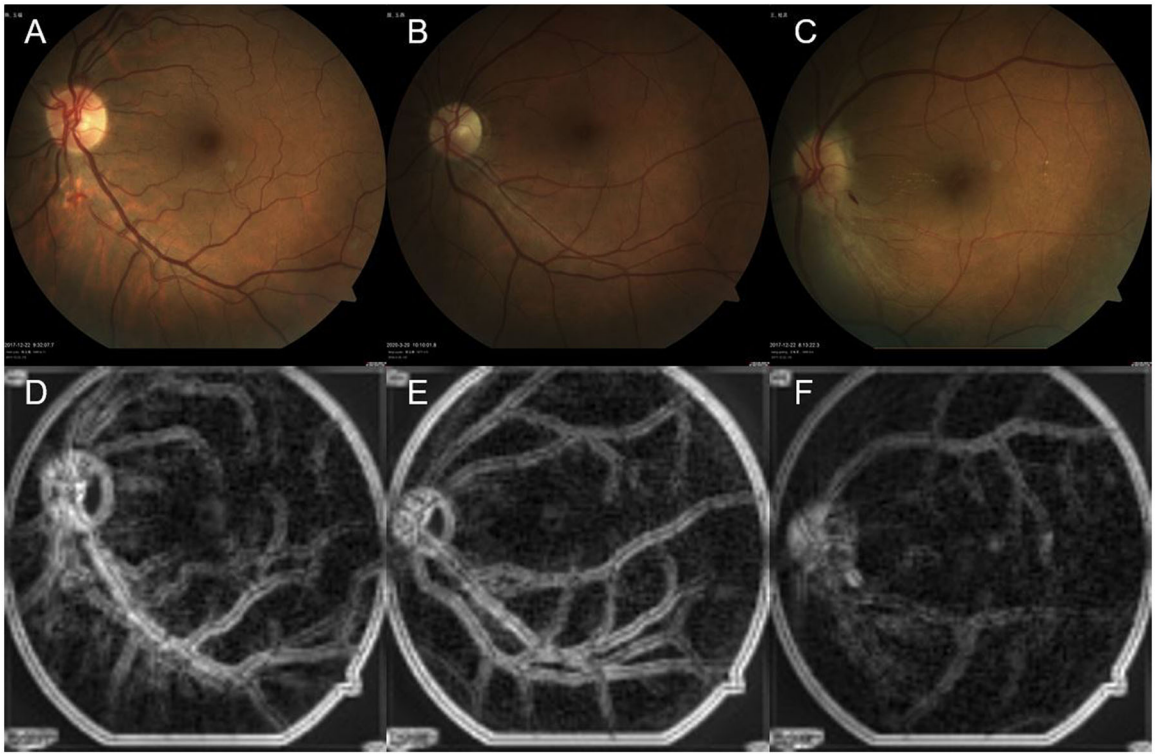


**Figure 4.** Comparison diagram of three types of feature fusion. D, E, and F are the feature fusion diagrams of A (normal), B (atrophy), and C (edema).

of networks has been a big problem for a long time. People may wonder how neural networks work to identify ocular fundus diseases. Therefore, CAM and feature fusion were chosen to find out the focus of ocular fundus and explain the mechanism of neural networks.

### CAM

CAM (Class Activation Mapping) is helpful to understand and analyze the working principle and decision process of neural network, which often used to visualize the importance of each location to the category, so CAM was used to locate the fundus lesion area.[19,20] First, made a GAP (global average pool) for the last feature map and calculated the average value of each channel. Then, mapped it to class score through FC layer to find out argmax and calculate the gradient of the largest class of output relative to the last feature map. Finally, visualized gradient on the original map to get the CAM.[17]

The first row of Figure 3 showed the original images of normal, atrophic and edema, respectively, and its CAMs were shown in the second row of Figure 3.

It could be seen from the figures that the neural network was mainly around the optic disk when making judgments. As shown in Figure 3(D), the red area of the CAM was close to the optic disk at the upper right of the optic disk.

Figure 3(E) the main red area of the CAM is at the right of the optic disk, and some red areas are in the optic disk, which is more obvious in Figure 3(F) that the whole red area almost coincides with the optic disk. While the macular region was not valued by the neural network. This indicated that the optic disk area was more important in judging the classification.

After image threshold processing, the low color temperature part was removed, and the attention space proportions of the image in the third line of Figure 3 were 0.88, 0.75, and 0.76, respectively. VGG16 had a wider range of attention than other neural networks, which probably provided the necessary support for its better effect.

### Feature fusion

VGG16 has 13 convolution layers. Feature fusion technology was used to visualize the neural network middle layer.[21–23] Feature fusion refers to the weighted average of features extracted by convolution kernel in the same layer to an image, which is the feature fusion image. Because the image resolution in the deep layer was too low, the feature fusion image of the third layer was selected for analysis (Figure 4).

Compared with normal disk and disk with atrophy, the optic disk area of ODE was seriously blurred as well as the blood vessels, making it easier to distinguish. These findings were also consistent with the most accurate image classification of ODE.

In the feature fusion image, the optic disk of normal and atrophy were similar, and the vascular part was significantly enhanced. Compared with normal images, the blood vessels of atrophy tended to be closer to the center of fundus, while the blood vessels of normal tended to be more evenly distributed. This was the feature of neural network convolution layer extraction, which helped us better understand what features neural network based on in distinguishing fundus images.

**Table 3.** Comparison of methods for fundus image classification.

| Reference | Pre-treatment | Classifier | Categories of classification | Characteristic | Insufficient |
|---|---|---|---|---|---|
| Rishab, 2017[6] | Rotation, brightness adjustment | Rerated CNN | Normal and DR | High sensitivity and specificity, visualization maps generated from deep features. | Not applicable to MESSIDOR 2 database |
| Jin, 2019[13] | Data augmentation (cropping corners and flipping) | Inception v3, VGG19, ResNet50 | Optic neuropathies, pseudopapilledema and normal | Bayesian optimization for hyper-parameter by Scikit-Optimize | Lack of interpretability analysis of neural networks |
| Lakshmana, 2021[8] | Image conversion, filtering, morphological operation, and segmentation | GLCM, GLRLM, Ridgelet Transform & SMO | Normal and DR | Extract and fuse the ophthalmoscopic features based on textural gray-level features | Using all textural and Ridgelet features may include irrelevant features for the task of DR recognition, which can incur larger computation time, and sometimes even reduce the recognition accuracy. |
| Sarmad, 2021[9] | Contrast limited adaptive histogram equalization method and 3D-CNN | Lutional Sparse Image Decomposition fusion method and extreme learning machine | Normal and DR | Pre-trained CNN model is used to extract features from the detected hemorrhages. | Execution time need to be reduced in the future work |
| Venkatesan, 2021[10] | Segmentation of the retinal layer and Global Weighted LBP supported Enhancement | Mayfly-Optimization Algorithm and Fine-Gaussian-SVM | Healthy and CNV | Extraction of handcrafted features (GLCM, Hu moments and LBP) and Feature reduction with MOA | Only limited images are considered for the assessment |
| Our proposed method | Image clipping, Gaussian blur and fusion, data augmentation | VGG16,VGG19, ResNet50, Inception v3 | ODE, optic atrophy and normal | Data augment method, Visualization of neural network | Only limited to one image dataset |

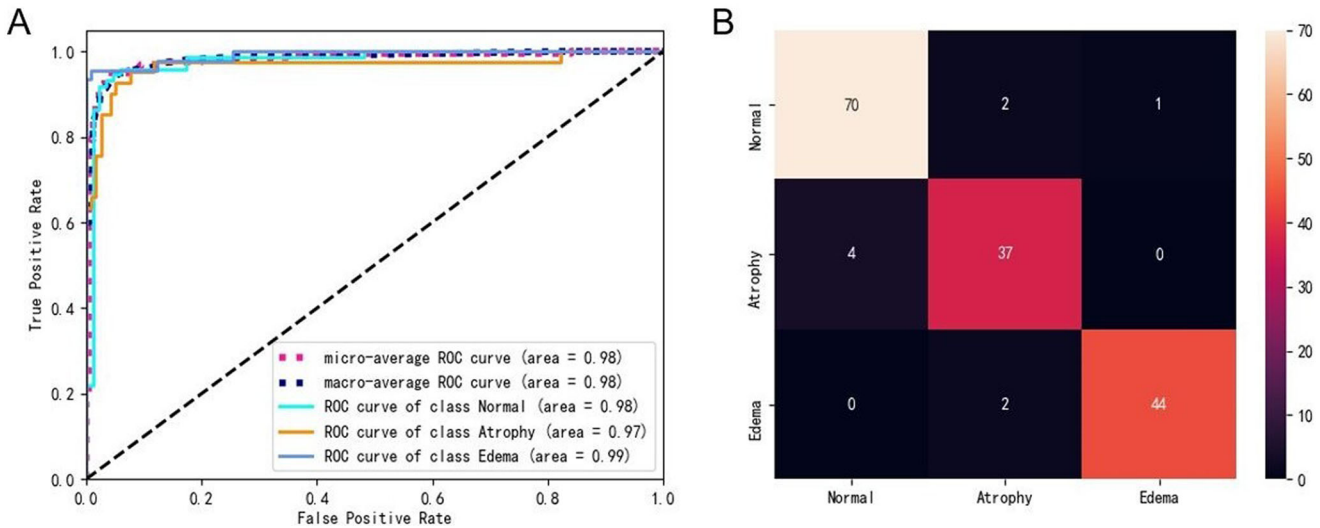


**Figure 5.** (A) Receiver operating characteristic curve. (B) Confusion matrix.

Convolution neural network extracted the key areas and ignored the unimportant areas through convolution pooling and other operations. For fundus images, it highlighted the spatial distribution and thickness of blood vessels, for making judgement. Through visualization, the key areas determined by neural network and what key information it extracted were analyzed, so as to realize the interpretability of neural network.

## Discussion

Compared with the methods with other paper's in the literature, we aimed to use image preprocessing and neural network to distinguish ODE, optic atrophy and normal images, which worked well and the performance of different neural network models was compared (Table 3). Besides, visualization was used to understand the internal principle of neural network and to find the region of interest of neural network.

But the method also had shortcomings that our classifier only focused on CNNs when we should combine them with traditional methods, in this way the performance would be better. The image dataset we used includes only 804 fundus images and we did not test our model on other datasets, which might cause our model not to be universal.

In our dataset, the number of different categories is similar, and the false-positive number in Figure 5 is small. But when it comes to a large number of healthy individuals such as medical examination, there will be lots of false-positive cases, which means that the automatic detection system cannot be used individually. While it can still be used as an auxiliary diagnosis for large medical examination and subsequent examinations.

## Conclusions

Neural network was applied to judge eye diseases and a set of image pre-processing and data enhancement methods were created which improve the accuracy of networks efficiently. CAMs were utilized to analyze the focus of networks and feature fusion to explore the mechanism of neural network. In future work, we will use neural network to diagnose more medical diseases, and make it easier for doctors to learn lesions and make judgments through the visualization process.

The visualization method of CAMs can be used to identify lesion area such as, diabetes retinopathy, age-related maculopathy, retinal vein occlusion for assisting doctors to make the judgment. Previous layers of the neural network can be used as a feature extractor for image pretreatment in corneal topography and other ophthalmic images. With the development of the neural network, Biomedical imaging will become more and more intelligent.

## Disclosure statement

No potential conflict of interest was reported by the author(s).

## Funding

This work was supported by Tianjin Health Research Project [No. ZC20166], Tianjin Key Medical Discipline(Specialty) Construction Project [No.TJYXZDXK-016A] and the Pilot Scheme of Talent Training in Basic Sciences (Boling Class of Physics, Nankai University), Ministry of Education.

## Data availability statement

Due to the nature of this research, participants of this study did not agree for their data to be shared publicly, so supporting data is not available.

## References

1. Sengupta A, Ye Y, Wang R, Liu C, Roy K. Going deeper in spiking neural networks: VGG and residual architectures. Front Neurosci. 2019;13(95):95.
2. Ioffe S, Szegedy C. Batch normalization: accelerating deep network training by reducing internal covariate shift//International conference on machine learning. PMLR. 2015:448–456.
3. He K, Zhang X, Ren S, Sun J. Deep residual learning for image recognition. Proceedings of the IEEE Conference on Computer Vision and Pattern Recognition (pp. 770–778), 2016.
4. Szegedy C, Vanhoucke V, Ioffe S, Shlens J. Rethinking the inception architecture for computer vision//Proceedings of the IEEE Conference on Computer Vision and Pattern Recognition (pp. 2818–2826), 2016.
5. Gulshan V, Peng L, Coram M, Stumpe MC, Wu D, Narayanaswamy A, Venugopalan S, Widner K, Madams T, Cuadros J, et al. Development and validation of a deep learning algorithm for detection of diabetic retinopathy in retinal fundus photographs. JAMA. 2016;316(22):2402–2410. doi:10.1001/jama.2016.17216.
6. Gargeya R, Leng T. Automated identification of diabetic retinopathy using deep learning. Ophthalmology. 2017;124(7):962–969. doi:10.1016/j.ophtha.2017.02.008.
7. Wang X, Ju L, Zhao X, Ge Z. Retinal abnormalities recognition using regional multitask learning. International Conference on Medical Image Computing and Computer-Assisted Intervention, Springer, Cham (pp. 30–38), 2019.
8. Ramasamy LK, Padinjappurathu SG, Kadry S, Damaševičius R. Detection of diabetic retinopathy using a fusion of textural and ridgelet features of retinal images and sequential minimal optimization classifier. PeerJ Comput Sci. 2021;7:e456. doi:10.7717/peerj-cs.456.
9. Maqsood S, Damaševičius R, Maskeliūnas R. Hemorrhage detection based on 3D CNN deep learning framework and feature fusion for evaluating retinal abnormality in diabetic patients. Sensors. 2021;21(11):3865. doi:10.3390/s21113865.
10. Rajinikanth V, Kadry S, Damaševičius R, Taniar D, Rauf HT. Machine-learning-scheme to detect choroidal-neovascularization in retinal OCT image//2021 Seventh International Conference on Bio Signals, Images, and Instrumentation (ICBSII), IEEE (pp. 1–5), 2021.
11. Krizhevsky A, Sutskever I, Hinton GE. ImageNet classification with deep convolutional neural networks. Commun Acm. 2017; 60(6):84–90. doi:10.1145/3065386.
12. Karpathy A, Toderici G, Shetty S, Leung T, Sukthankar R, Fei-Fei L. Large-scale video classification with convolutional neural networks. Proceedings of the IEEE Computer Society Conference on Computer Vision and Pattern Recognition (pp. 1725–1732), Columbus, OH, 2014.
13. Ahn JM, Kim S, Ahn KS, Cho S, Kim US. Accuracy of machine learning for differentiation between optic neuropathies and pseudopapilledema. BMC Ophthalmol. 2019; 19(1):7. doi:10.1186/s12886-019-1184-0.
14. Dietterich T. Overfitting and undercomputing in machine learning. ACM Comput Surv. 1995;27(3):326–327. doi:10.1145/212094.212114.
15. Wong SC, Gatt A, Stamatescu V, McDonnell MD. Understanding data augmentation for classification: when to warp? 2016 International Conference on Digital Image Computing: Techniques and Applications (DICTA) (pp. 1–6), Gold Coast, Australia: IEEE, 2016.
16. George D, Shen H, Huerta EA. Deep Transfer Learning: A new deep learning glitch classification method for advanced LIGO. ArXiv preprint arXiv:2017, 1706.07446, 2017.
17. Lin TY, Goyal P, Girshick R, He K, Dollar P. Focal loss for dense object detection. Proceedings of the IEEE International Conference on Computer Vision (pp. 2980–2988), Venice, Italy, 2017.
18. Kingma DP, Ba J. Adam: A method for stochastic optimization. ArXiv preprint arxiv:2014, 1412.6980, 2014.
19. Zhou B, Khosla A, Lapedriza A, Aude O, Torralba A. Learning deep features for discriminative localization. Proceedings of the IEEE Conference on Computer Vision and Pattern Recognition (pp. 2921–2929), 2016.

20. Selvaraju RR, Cogswell M, Das A, Vedantam R, Parikh D, Batra D. Grad-Cam: visual explanations from deep networks via gradient-based localization. Proceedings of the IEEE International Conference on Computer Vision (pp. 618–626), Venice, Italy, 2017.
21. Zeiler MD, Fergus R. Visualizing and understanding convolutional networks//European conference on computer vision. Springer, Cham. 2014; p. 818–833.
22. Simonyan K, Vedaldi A, Zisserman A. Deep inside convolutional networks: Visualising image classification models and saliency maps. ArXiv preprint arxiv:2013, 1312.6034, 2013.
23. Jiang PT, Zhang CB, Hou Q, Cheng MM, Wei Y. Layercam: exploring hierarchical class activation maps for localization. IEEE Trans Image Process. 2021;30:5875–5888. doi:10.1109/TIP.2021.3089943.